7.3. Thermal neutron detection

BY P. CONVERT AND P. CHIEUX

7.3.1. Introduction

In this chapter, we shall be concerned with the detection of neutrons having thermal and epithermal energies in the range 0.0002–10 eV (20–0.1 Å). Given the cost and the rarity of the neutron sources, it is clear that the recent trends in neutron diffractometry are more and more in the direction of designing new instruments around highly efficient and complex detection systems. These detection systems become more and more adapted to the particular requirements of the different experimental needs (counting rate, size, resolution, definition, shielding and background, TOF, *etc*.). It is therefore difficult to speak about neutron detectors and intensity measurements as such without reference to the complete spectrometers, and this should include the on-line computer.

Most neutron detectors for research experiments have been created and developed using fission reactors as neutron sources [*i.e.* with an upper limit of usable energy of 0.5 eV (0.4 Å)]. Given the relatively low intensity of reactor neutron beams, a very successful effort has been made to increase the detector efficiency and the detection area as much as possible. The recent construction of pulsed neutron sources extends the range of incident energy to at least 10 eV and generalizes the use of time-of-flight (TOF) techniques. A broad range of fully operational neutron detectors, well adapted to reactors as neutron sources, is commercially available, but this is not yet the case for pulsed sources. Probably due to the variation of intensity of the early neutron beams, it is a tradition in neutron research to monitor the incident flux with a low-efficiency detector, which in the best case has a stability of the order of 10^{-3}, *i.e.* sufficient for most experiments.

7.3.2. Neutron capture

Neutrons' lack of charge and the fact that they are only weakly absorbed by most materials require specific nuclear reactions to capture them and convert them into detectable secondary particles. Table 7.3.2.1 lists the neutron-capture reactions that are commonly used in thermal neutron detection. The incoming thermal neutron brings a negligible energy to the nuclear reaction, and the secondary charged particles or fission fragments are emitted in random directions following the conservation-of-momentum law $\sum m_i v_i = 0$. The capture or absorption cross sections for a number of nuclei of interest are plotted as a function of neutron energy in Fig. 7.3.2.1. These cross sections are commonly expressed in barns (1 barn = 10^{-28} m^2). At low energies, they are inversely proportional to neutron velocity, except in the case of Gd, which has a nuclear resonance at 0.031 eV. The total efficiency ε of neutron detection can be expressed by the equation

$$\varepsilon = \xi[1 - \exp(-N\sigma_a t)], \qquad (7.3.2.1)$$

where N is the number of absorbing nuclei per unit volume, σ_a is their energy-dependent absorption cross section, and t is the thickness of the absorbing material. The factor $1 - \exp(-N\sigma_a t)$ gives the neutron-capture efficiency, while ξ is a factor ≤ 1 that depends on the detector geometry and materials (absorption and scattering in the front window) and on the efficiency of the secondary particles.

7.3.3. Neutron detection processes

A detection process consists of a chain of events that begins with the neutron capture and ends with the macroscopic 'visualization' of the neutron by a sensor (electronic or film). The quality of a detection process will depend on the efficiency of the conversion steps and on the characteristics of the emission steps, which alternate in the process (see Table 7.3.3.1). We present below typical detection processes.

7.3.3.1. *Detection via gas converter and gas ionization: the gas detector*

The neutron capture and the trajectories of the secondary charged particles as well as the specific gas ionization along these trajectories are presented in Figs. 7.3.3.1(*a*) and (*b*). Since the gas ionization energy is about 30 eV per electron (42 eV for ^{3}He and 30 eV for CH_4), there are about 25 000 ion pairs (e^-, He^+ or e^-, CH_4^+) per captured neutron. Gases such as CH_4 or C_3H_8 are added to diminish the length of the trajectories, *i.e.* the wall effect [see Subsection 7.3.4.2(*b*)].

We give in Fig. 7.3.3.1(*c*) the proton range of an ^{3}He neutron-capture reaction in various gases (Fischer, Radeka, & Boie, 1983). A schematic drawing of a gas monodetector, which might be mounted either in axial or in radial orientation in the neutron beam, is given in Fig. 7.3.3.1(*d*).

For this type of detector, the efficiency as a function of the gas pressure, or gas-detector law, is written as

$$\varepsilon(\lambda) = \xi[1 - \exp(-bPt\lambda)],$$

with P (atm) = the detector-gas pressure at 293 K, t (cm) = the gas thickness, and λ (Å) = the detected neutron wavelength. The numerical coefficient b, obtained at 293 K from the ideal gas law, the Avogadro number N_A, and the gas absorption cross section σ_a (barns) at $\lambda_0 = 1.8$ Å, is

$$b = \frac{273}{293} \times \frac{N_A}{22\,414} \times \frac{\sigma_a}{\lambda_0}.$$

For ^{3}He, with $\sigma_a = 5333$ barns at $\lambda_0 = 1.8$ Å, $b = 0.07417$; for $^{10}BF_3$, with $\sigma_a = 3837$ barns at $\lambda_0 = 1.8$ Å, $b = 0.0533$. We give in Table 7.3.3.2 a few examples of gas-detector characteristics.

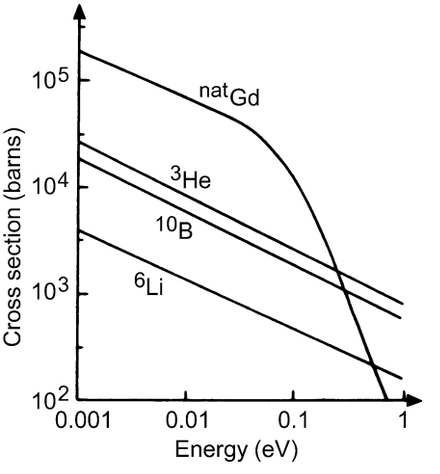

Fig. 7.3.2.1. The capture cross sections for a number of nuclei used in neutron detection. [Adapted from Convert & Forsyth (1983).]

references